TU Delft

Delft University of Technology

Sensory contributions to stabilization of trunk posture in the sagittal plane

van Dieën, Jaap H.; van Drunen, Paul; Happee, Riender

DOI
10.1016/j.jbiomech.2017.07.016

Publication date
2017

Document Version
Accepted author manuscript

Published in
Journal of Biomechanics

Citation (APA)
van Dieën, J. H., van Drunen, P., & Happee, R. (2017). Sensory contributions to stabilization of trunk posture in the sagittal plane. *Journal of Biomechanics*, *70 (2018)*, 219-227. https://doi.org/10.1016/j.jbiomech.2017.07.016

Important note
To cite this publication, please use the final published version (if applicable).
Please check the document version above.

Copyright
Other than for strictly personal use, it is not permitted to download, forward or distribute the text or part of it, without the consent of the author(s) and/or copyright holder(s), unless the work is under an open content license such as Creative Commons.

Takedown policy
Please contact us and provide details if you believe this document breaches copyrights.
We will remove access to the work immediately and investigate your claim.

This work is downloaded from Delft University of Technology.
For technical reasons the number of authors shown on this cover page is limited to a maximum of 10.

Accepted Manuscript

Sensory contributions to stabilization of trunk posture in the sagittal plane

Jaap H. van Dieën, Paul van Drunen, Riender Happee

PII: S0021-9290(17)30375-5
DOI: http://dx.doi.org/10.1016/j.jbiomech.2017.07.016
Reference: BM 8304

To appear in: *Journal of Biomechanics*

Accepted Date: 16 July 2017

Please cite this article as: J.H. van Dieën, P. van Drunen, R. Happee, Sensory contributions to stabilization of trunk posture in the sagittal plane, *Journal of Biomechanics* (2017), doi: http://dx.doi.org/10.1016/j.jbiomech.2017.07.016

This is a PDF file of an unedited manuscript that has been accepted for publication. As a service to our customers we are providing this early version of the manuscript. The manuscript will undergo copyediting, typesetting, and review of the resulting proof before it is published in its final form. Please note that during the production process errors may be discovered which could affect the content, and all legal disclaimers that apply to the journal pertain.

ACCEPTED MANUSCRIPT

Sensory contributions to stabilization of trunk posture in the sagittal plane

Jaap H. van Dieën[1]; Paul van Drunen[2]; Riender Happee[2]

[1]Department of Human Movement Sciences, Vrije Universiteit Amsterdam, Amsterdam Movement Sciences, Amsterdam, The Netherlands
[2]BioMechanical Engineering, Faculty of Mechanical, Maritime and Materials Engineering (3ME), Delft University of Technology, The Netherlands

word count: 3473 (max 3500)

running head: sensory feedback in trunk stabilization

corresponding author:
prof.dr. Jaap H. van Dieën
Department of Human Movement Sciences
VU University Amsterdam
van der Boechorststraat 9
NL-1081 BT Amsterdam
Netherlands
t: (31) 20 5988501, e: j.van.dieen@vu.nl

ACCEPTED MANUSCRIPT

ACCEPTED MANUSCRIPT

Abstract

Trunk stabilization is required to control posture and movement during daily activities. Various sensory modalities, such as muscle spindles, Golgi tendon organs and the vestibular system, might contribute to trunk stabilization and our aim was to assess the contribution of these modalities to trunk stabilization. In 35 healthy subjects, upper-body sway was evoked by continuous unpredictable, force-controlled perturbations to the trunk in the anterior direction. Subjects were instructed to either 'maximally resist the perturbation' or to 'relax but remain upright' with eyes closed. Frequency response functions (FRFs) of admittance, the amount of movement per unit of force applied, and reflexes, the modulation of trunk extensor activity per unit of trunk displacement, were obtained. To these FRFs, we fitted physiological models, to estimate intrinsic trunk stiffness and damping, as well as feedback gains and delays. The different model versions were compared to assess which feedback loops contribute to trunk stabilization. Intrinsic stiffness and damping and muscle spindle (short-delay) feedback alone were sufficient to accurately describe trunk stabilization, but only with unrealistically low reflex delays. Addition of muscle spindle acceleration feedback or inhibitory Golgi tendon organ feedback yielded realistic delays and improved the model fit, with a significantly better model fit with acceleration feedback. Addition of vestibular feedback did not improve the model fit. In conclusion, muscle spindle feedback and intrinsic mechanical properties are sufficient to describe trunk stabilization in the sagittal plane under small mechanical perturbations, provided that muscle spindles encode acceleration in addition to velocity and position information.

Keywords: spine, postural control, system identification, feedback

ACCEPTED MANUSCRIPT

ACCEPTED MANUSCRIPT

Introduction

Trunk stabilization can be defined as maintaining control over trunk posture and movement, in spite of the disturbing effects of gravity and mechanical perturbations. In many daily-life activities, the trunk resembles an inverted pendulum that is continuously perturbed by small disturbances, due to reaction forces caused by for example breathing (Smith et al., 2005) or arm movements (Hodges et al., 1999). Accurate control of trunk posture is required, for example, to allow hand movement with some degree of precision (Kaminski et al., 1995; Pigeon et al., 2000). How this stabilization is achieved is to a large extent unknown. Here, we specifically focus on control of an upright, unsupported trunk posture under low-force perturbations, a situation that is representative for many daily activities.

To adapt the degree of precision with which upright trunk posture is controlled, feedback gains appear to be modulated rather than the level of co-contraction (Willigenburg et al., 2010). This suggests dominance of feedback control in this regard and information providing feedback on trunk posture could be derived from several sensory modalities. Manipulation of sensory inputs has demonstrated that proprioceptive, vestibular and visual information can all contribute (Andreopoulou et al., 2015 ; Goodworth and Peterka, 2009; Maaswinkel et al., 2014; Willigenburg et al., 2012), but such manipulations cannot elucidate whether and how much these modalities contribute in conditions that are representative for daily activities.

We have recently developed a system identification technique, based on unpredictable force disturbances that cause small-amplitude perturbations of trunk posture (< 2.5 degree lumbar rotations), to identify contributions of different sources of feedback to trunk stabilization (van Drunen et al., 2013; van Drunen et al., 2014). This method relies on fitting a physiological model encompassing various sensory feedback loops to frequency responses of trunk displacement and trunk muscle electromyography (EMG) to low-amplitude force disturbances. Using this technique, trunk position and velocity encoded by muscle spindles (MS) were found to be the dominant sources of feedback for stabilization of the trunk (van Drunen et al., 2013; van Drunen et al., 2014). However, in these experiments, subjects were required to keep their hands on their head; a posture which likely entailed activity of shoulder and trunk muscles, which would increase the contribution of intrinsic muscle stiffness and damping to stabilization and, consequently, may have masked contributions of other sources of feedback.

Previous studies using system identification have indicated that several other feedback mechanisms may play a role in stabilization of posture in addition to position and velocity feedback by muscle spindles. Inclusion of spindle acceleration feedback (de Vlugt et al., 2006; Schouten et al., 2008a) and of excitatory feedback by Golgi tendon organs (GTO) (Mugge et al., 2010; Mugge et al., 2009) improved the model fit to measured arm admittance. In addition, visual and vestibular feedback were shown to contribute to frontal plane trunk stabilization (Goodworth and Peterka, 2009). However, other studies showed that the visual contribution to control of upright sitting without external perturbations or under anterior directed perturbations is not significant (Maaswinkel et al., 2015; Maaswinkel et al., 2014).

The aim of the present study was to assess the additional contribution to MS velocity and position feedback of acceleration feedback by MS, inhibitory and excitatory force feedback by GTO, and acceleration feedback by the vestibular organ to trunk postural control in an upright, unsupported posture with eyes closed and arms crossed over the chest, during low force perturbations. To this end, models representing various combinations of the mentioned feedback

ACCEPTED MANUSCRIPT

loops in addition to intrinsic mechanical parameters and MS position and velocity feedback were fitted to experimental data. Subsequently, the variance accounted for of trunk displacement and of trunk muscle EMG was assessed. Finally, the effect of feedback parameters on trunk stabilization in selected models was assessed.

Methods

Thirty-five participants (16 females, 19 males; body mass: 70 SD 13 kg; height 1.75 SD 0.09 m; age 36 SD 17 yrs) volunteered for this experiment. Participants did not report any disorders or use of medication that could affect balance control, nor any low-back pain in the 12 months prior to the experiments. All participants signed an informed consent and the protocol had been approved by the Ethics committee for Movement Sciences at the Vrije Universiteit Amsterdam (ECB 2015-18).

For the measurement, participants were seated in a kneeling-seated posture with their pelvis restrained (Figure 1). Force perturbations were applied in the anterior direction at the level of the 10^{th} thoracic vertebra by a magnetically driven linear actuator (Servotube STB2510S Forcer and Thrustrod TRB25-1380, Copley Controls, USA), with a thermoplastic patch (40x40x3mm) placed between the subject and the actuator to improve force transfer and comfort. Subjects were instructed to keep their eyes closed and arms crossed in front of the chest and to 'maximally resist the perturbation' by minimizing flexion/extension excursions (resist task), or to 'relax but remain sitting upright' (relax task). Tasks were performed in random order and repeated three times. Each trial had a duration of 50s. The perturbation force increased linearly from 0 to 60 N over 3 seconds, which was followed by a crested multi-sine signal (Pintelon and Schoukens, 2001), containing power at 8 paired frequencies, which were logarithmically distributed within a bandwidth of 0.2-15 Hz, with a peak amplitude of 35 N superimposed on the 60 N baseline preload.

The actuator's target force, displacement and the contact force between the actuator and subject were recorded at 400 samples/s. EMG of the lumbar part of the Longissimus muscle was measured bilaterally (REFA, TMSi, Netherlands), using single-use, adhesive electrodes (Blue Sensor N, Ambu A/S, Ballerup, Denmark) placed over the muscle bellies 3 cm lateral to interspinous space between L4 and L3. The EMG signals were sampled at 2000 samples/s. The Longissimus muscle was chosen because of the high coherence between this muscle's activity and thorax displacement (van Drunen et al., 2013). EMG signals were band-pass filtered 5 – 400 Hz (2^{nd} order Butterworth), rectified and averaged between left and right muscles.

All data processing and system identification were performed using custom-made software (The Mathworks, Inc., Natick, MA, United States). Closed loop identification (van Drunen et al., 2013; van Drunen et al., 2014) was used to describe the translational low-back admittance and reflexes as frequency response functions (FRFs). The admittance FRF describes the actuator displacement relative to the contact force, representing the inverse of low-back mechanical impedance, or in other words the resistance against the perturbation as a function of frequency. The reflex FRF describes the EMG amplitude modulation of the lumbar part of the Longissimus muscle relative to the actuator displacement. Coherences for admittance and reflex FRFs were assessed for the frequencies containing power in the perturbation signal.

The FRFs of the three repeated trials were weighted for coherence and averaged to obtain inputs for the parametric identification. Eight versions of a linear neuromuscular control model (Figure 2) were constructed to identify parameters representing intrinsic and reflexive contributions

ACCEPTED MANUSCRIPT

to trunk stabilization (Table 1), using parametric identification (Schouten et al., 2008a; van der Helm et al., 2002; van Drunen et al., 2013) separately for each participant and the two tasks. In all model versions, a single parameter was estimated to scale EMG amplitude to force. Muscle activation dynamics (H_{act}) was implemented as a second order system (Bobet and Norman, 1990) with a cut-off frequency (f_{act}) and a dimensionless damping (d_{act}), set to 0.75 Hz and 1.05, respectively, as the average activation dynamics in (van Drunen et al., 2013; van Drunen et al., 2014). Contact dynamics between the participant's trunk and the actuator was described by a parallel spring and damper (k_c, b_c) that were estimated assuming constant values over the two tasks. The stabilizing properties of passive tissues and muscle co-contraction and the destabilizing effect of trunk weight were lumped into two parameters describing the overall stiffness and damping (k_{eff}, b) of the low back, which were estimated for each task separately. The MS reflexive contribution was described by acceleration, velocity and position feedback gains (k_A, k_V, k_P) for each task specifically, with a common time delay (τ_{MS}). GTO feedback was described by a force feedback gain (k_{GTO}) for each task, with a single delay (τ_{GTO}). Finally, vestibular feedback was estimated by acceleration feedback gains (k_{VES}) for each task separately, and a single delay (τ_{VES}). Upper and lower bounds of estimated parameters are given in Table 2. More detailed information on the system identification approach has been reported previously (van Drunen et al., 2013; van Drunen et al., 2014). Different from these previous reports, model fitting was performed here by simulated annealing (Goffe, 1996), to ensure convergence of model estimates.

To assess the validity of the optimized models and their parameters, first, stability of the resulting models was assessed by checking for non-negative poles for the two tasks. For models producing stable results, estimated delays were assessed and the variance accounted for (*VAF*) in the time domain was used to compare the experimental measurements *x(t),* representing trunk displacement or EMG amplitude in either of the two tasks with the model outcomes $\hat{x}(t)$:

$$VAF_x = \left[1 - \frac{\sum_1^n (x(t_n) - \hat{x}(t_n))^2}{\sum_1^n (x(t_n))^2}\right] \cdot 100\% \qquad (1)$$

with *n* the number of data points in the signals. A *VAF* of 100% reflects a perfect replication of the measured signal by the model. *VAFs* were compared using non-parametric Wilcoxon matched pairs tests, between the reference model containing only MS velocity and position feedback and between all alternative more comprehensive models.

For the models producing the best fit to the data with realistic delay estimates, sensitivity of model outcomes to parameters was assessed comparing trunk displacement and trunk muscle activity predicted with the median, 25th and 75th percentile values of the model parameters concerned.

Results

We parameterized eight model versions representing different combinations of sensory feedback in trunk stabilization (Table 1). Optimized models containing GTO feedback produced unstable results in 6 to 23 of 35 participants, depending on the type of model. GTO gains were distributed around zero and unstable results were associated with negative estimates of GTO feedback gains, which

ACCEPTED MANUSCRIPT

reflect positive force feedback. We, therefore, reran the analysis with a lower boundary on GTO gains of 0.

Inclusion of MS acceleration feedback (MS_A), generally improved *VAFs* in comparison with the reference model (MS velocity and position feedback only) and with other models without MS_A (Table 3 and Figure 3). Importantly, inclusion of MS_A changed MS feedback delays substantially. In the reference model, estimates were often at the lower boundary of 5 ms with a median of 7 ms. With inclusion of MS_A, MS delays were estimated at median values from 36 to 39 ms (Figure 4).

Inclusion of inhibitory GTO feedback increased reflex *VAFs* relative to the reference model, but not relative to models including MS_A (Table 3 and Figure 3). Inclusion of GTO feedback affected estimates of MS delays in a similar way as inclusion of MS_A, although estimates were slightly lower with medians from 23 to 36 ms (Figure 4). Simultaneous identification of MS_A and inhibitory GTO feedback led to very low GTO delays (Figure 4).

Inclusion of VES feedback improved only the *VAF* of the admittance in the resist task and these effects were smaller than 1% (Table 3 and Figure 3). In absence of MS_A or GTO feedback, VES feedback led to MS delays close to the lower boundary of 5 ms (Figure 4). In addition, delay estimates for vestibular feedback approached upper boundaries of 200 ms when VES was combined with MS_A (Figure 4).

Estimates of other model parameters are shown in supplementary material. Predictably, inclusion of inhibitory GTO feedback caused increases of estimates of MS gains, most notably of MS position feedback (Figure S.1). Parameters reflecting intrinsic trunk properties and contact dynamics were fairly consistent between models (Figure S.2). Estimates of effective mass were generally moderately correlated to, but lower than, anthropometric estimates of upper body mass (Figure S.3).

In conclusion, substantial improvements in *VAFs*, without yielding unrealistic delay estimates, were achieved with inclusion of MS_A or inhibitory GTO feedback, with the former providing the highest *VAFs*. Models combining MS_A, GTO and VES feedback did not lead to clear further improvements in *VAF* or yielded unrealistic reflex delays. An illustration of the goodness of fit of the MS_A model is given in Figure 5.

Comparison of FRFs based on median, 25^{th} and 75^{th} percentiles of the acceleration feedback gain shows that acceleration feedback gain had strong effects on reflex gain and phase above 1 Hz (Figure 6). However, this did not strongly affect mechanical admittance, due to the inertia of the trunk and the low-pass filtering properties of the activation dynamics (H_{act}). While the effect of acceleration feedback on the admittance FRFs was limited, inclusion of acceleration feedback substantially affected estimates of MS feedback delays (Figure 4). As described above, without acceleration or force feedback, MS delay estimates tended towards the lower boundary of 5 ms, while the median estimate of the MS_A model was 37 ms. Using this median delay of the MS_A model in a model without acceleration feedback did appreciably increase admittance around 1 Hz, particularly in the resist task (Figure 6). This suggests that with feedback delays of around 30 ms, the high-frequency response provided by acceleration feedback is useful to attenuate oscillations in this frequency range.

Discussion

ACCEPTED MANUSCRIPT

The aim of this study was to assess contributions of MS acceleration feedback, GTO force feedback, and VES acceleration feedback, in addition to MS velocity and position feedback, to the stabilization of unsupported upright trunk posture under low-amplitude perturbations. The results indicate that in addition to MS feedback of position and velocity, MS feedback of acceleration (MS_A) plays a role in trunk stabilization. No indications were found for contributions of excitatory GTO and VES feedback. Inhibitory GTO feedback did improve model fit but to a lesser extent than MS_A feedback.

Measurements of MS afference support the notion that MS may encode acceleration (Dimitriou and Edin, 2008; Henatsch, 1971; Schafer and Kijewski, 1974) and it has been shown that acceleration feedback would simplify control of upright standing (Insperger et al., 2013). Furthermore, muscle activation patterns following perturbations of whole-body balance were in line with predictions of a control model including acceleration feedback (Welch and Ting, 2008, 2009). The presence of MS_A was supported here by significantly better *VAFs* of models with than without MS_A. The better fit obtained with MS_A concurs with our previous work (Table 2 in van Drunen et al. (2014)) and was now proven to be significant. Previously, we may have missed effects of MS_A, due to low statistical power and a high intrinsic stiffness given the posture in which subjects were tested.

Excitatory GTO feedback was found to cause instability of trunk posture. In contrast, excitatory GTO feedback has been reported to contribute to stabilization of arm posture. However, the most pronounced contribution was found when the hand interacted with an object that provided considerable resistance against movement (Mugge et al., 2009). For the trunk, this might resemble control of a supported trunk posture, as when leaning against a chair back, but this may not generalize to unsupported postures. GTO feedback may also contribute indirectly to position, velocity or acceleration feedback, as it can resolve ambiguities in MS afference that arise from tendon compliance leading to independency between MS length and joint angle (Dimitriou and Edin, 2010; Kistemaker et al., 2013). This aspect of GTO feedback would not be captured by the models applied here.

Inhibitory GTO feedback increased reflex *VAFs* by a better fit at higher frequencies, but it did not improve admittance *VAFs* and improvements were smaller than for MS_A feedback. When lying prone, GTO feedback in the triceps surae muscle is inhibitory; when standing this inhibition is reduced (Faist et al., 2006; Horslen et al., 2017). Possibly the upright posture and the average forward loading in our test conditions minimized GTO gains. Inhibitory GTO feedback acts as a high-pass filter on force output of the muscle (Schouten et al., 2008b). The high-pass filtering effect of inhibitory force feedback requires an increase of MS (or VES) gains proportional to the GTO gain to keep average muscle force constant, as was reflected in the parameter estimates (Figure S.1). Acceleration feedback also increases the high-frequency content of the muscle force, given the higher frequency content of acceleration compared to velocity and position. Therefore, it cannot be excluded that GTO and acceleration feedback are simultaneously present. The similarity of their effect on muscle force may make it impossible to obtain reliable identification of both simultaneously.

No evidence for a contribution of VES acceleration feedback to trunk stabilization was found in the present study. In contrast, system identification by Goodworth and Peterka (2009) indicated an important contribution of VES feedback to frontal trunk stabilization, which increased with perturbation amplitude. However, subjects were placed on a moving support surface, while surface instability has been shown to lead to increased VES feedback in frontal plane trunk control (Andreopoulou et al., 2015). Here all tests were performed on a rigid support surface, under small amplitude perturbations, conditions that were chosen as representative for functional tasks. In

ACCEPTED MANUSCRIPT

addition, differences between frontal plane and sagittal plane stabilization may account for this disparity, since our recent work suggested very limited contributions of VES feedback to sagittal plane stabilization even on a moving surface (van Drunen et al., 2015; van Drunen et al., 2016). Finally, Goodworth and Peterka (2009) modelled the VES contributions as velocity feedback, whereas we modelled the VES contribution as acceleration feedback. The vestibular system encodes linear acceleration by otolith afferents and angular velocity by semicircular canal afferents (Angelaki and Cullen, 2008). In previous studies using platform induced perturbations, we found that head rotations were negligible relative to upper body rotations, while head translations were more substantial (van Drunen et al., 2015; van Drunen et al., 2016). This suggests limited input to the semicircular canals compared to the otoliths, especially when considering the detection thresholds of these sub-systems (Sadeghi et al., 2007; Yu et al., 2012).

In the present study, subjects had their eyes closed and visual feedback was ruled out. Previously using the same set-up as used in the current study no differences were found in FRFs between eyes open and eyes closed conditions (Maaswinkel et al., 2015). However, that study used a resist task only and a visual contribution in a relax task can thus not be excluded. However, removal of visual feedback did not increase trunk sway in upright unsupported and unperturbed sitting (Maaswinkel et al., 2014). Consequently, a substantial contribution of visual feedback in tasks such as tested here appears unlikely.

When no acceleration or GTO feedback is present, feedback delays of position and velocity feedback need to be very short to achieve the admittance observed in the present study. The median feedback delay estimated for the MS model was 7 ms, while including acceleration or GTO feedback it was estimated at 37 and 28 ms, respectively. The latter values are in line with previous system identification estimates (Goodworth and Peterka, 2009; van Drunen et al., 2013; van Drunen et al., 2014). However, EMG responses in trunk extensor muscles after transient perturbations were found to occur at two latencies ranging from 9-20 and 30-50 ms, respectively (Dimitrijevic et al., 1980; Tani et al., 1997; Zedka et al., 1999). So, while shorter delays than estimated with the MS_A and GTO models cannot be ruled out, the delays estimated with the MS (and MS+VES) model appeared too short. With a reflex delay of around 30 ms, the high-frequency response provided by positive acceleration or negative force feedback are needed to attenuate perturbations with a frequency content between 1 and 2 Hz.

In the models used, trunk movement was described in terms of translation, since we previously showed that the effective rotation point was not well defined and inconsistent over subjects and tasks (van Drunen et al. 2013). However, the destabilizing effect of gravity was taken into account, as lumped with the intrinsic stiffness. The simplification to a translational model thus ignores only the height of the upper body centre of mass and the arm of the actuator above the centre of rotation. The actuator used to perturb trunk posture may have provided some tactile information used to control trunk posture, but this was unlikely to completely efface the effects of other sensory inputs (Maaswinkel et al., 2014). As in many daily life activities, pressure distribution on the seat may have provided a source of sensory information that was not taken into account. Finally, we addressed stabilization in the sagittal plane only. A strength of this study was that we tested a large group of participants with a wide age range (19-67 years). Hence, the results can be considered representative for healthy adults. The results may not generalize to individuals with disorders, for example, changes in sensory weighting for trunk control have been shown in patients with vestibular disorders (Goodworth and Peterka, 2010) and in patients with back pain (Claeys et al., 2011; Willigenburg et al., 2013).

ACCEPTED MANUSCRIPT

In conclusion, the results of the present study indicate that in addition to MS feedback of position and velocity, MS feedback of acceleration plays a role in sagittal plane trunk stabilization. Despite the finding that effects of changes in acceleration gains on kinematics were limited due to the low-pass filtering properties of the series elasticity in the trunk muscle-joint system and of trunk inertia, they were deemed relevant, since at perturbation frequencies between 1 and 2 Hz position and velocity feedback appeared too slow. This would imply functional relevance of acceleration feedback, since admittance is maximal in this frequency range.

Acknowledgements

The authors would like to thank Mariette Griffioen, Jeffrey Warmerdam and Drs. Erwin Maaswinkel and Matej Voglar for help in data collection and Dr. Huub Maas for reviewing a draft version of this paper. The study was partially supported by the Dutch Technology Foundation STW, which is part of the Netherlands Organization for Scientific Research (NWO), and which is partly funded by the Ministry of Economic Affairs. See www.neurosipe.nl - Project 10732: QDISC.

Conflict of interest

The authors have no conflict of interest to report.

References

Andreopoulou, G., Maaswinkel, E., Cofre Lizama, L.E., van Dieen, J.H., 2015. Effects of support surface stability on feedback control of trunk posture. Exp Brain Res 233, 1079-1087.

Angelaki, D.E., Cullen, K.E., 2008. Vestibular system: the many facets of a multimodal sense. Annu Rev Neurosci 31, 125-150.

Bobet, J., Norman, R.W., 1990. Least-squares identification of the dynamic relation between the electyromyogram and joint moment. Journal of Biomechanics 23, 1275-1276.

Claeys, K., Brumagne, S., Dankaerts, W., Kiers, H., Janssens, L., 2011. Decreased variability in postural control strategies in young people with non-specific low back pain is associated with altered proprioceptive reweighting. Eur J Appl Physiol 111, 115-123.

de Vlugt, E., Schouten, A.C., van der Helm, F.C.T., 2006. Quantification of intrinsic and reflexive properties during multijoint arm posture. Journal of Neuroscience Methods 155, 328-349.

Dimitrijevic, M.R., Gregoric, M.R., Sherwood, A.M., Spencer, W.A., 1980. Reflex responses of paraspinal muscles to tapping. J Neurol Neurosurg Psychiatry 43, 1112-1118.

Dimitriou, M., Edin, B.B., 2008. Discharges in human muscle receptor afferents during block grasping. J Neurosci 28, 12632-12642.

Dimitriou, M., Edin, B.B., 2010. Human muscle spindles act as forward sensory models. Curr Biol 20, 1763-1767.

ACCEPTED MANUSCRIPT

Faist, M., Hoefer, C., Hodapp, M., Dietz, V., Berger, W., Duysens, J., 2006. In humans Ib facilitation depends on locomotion while suppression of Ib inhibition requires loading. Brain Res 1076, 87-92.

Goffe, W.L., 1996. SIMANN: A Global Optimization Algorithm using Simulated Annealing. Studies in Nonlinear Dynamics and Econometrics 1, 169-176.

Goodworth, A.D., Peterka, R.J., 2009. Contribution of sensorimotor integration to spinal stabilization in humans. J Neurophysiol 102, 496-512.

Goodworth, A.D., Peterka, R.J., 2010. Influence of bilateral vestibular loss on spinal stabilization in humans. J Neurophysiol 103, 1978-1987.

Henatsch, D., 1971. Pro und Contra zur Beschleunigungsempfindlichkeit der Muskelspindeln. Bull schweiz Akad med Wiss 27, 266-281.

Hodges, P.W., Cresswell, A.G., Thorstensson, A., 1999. Preparatory trunk motion accompanies rapid upper limb movement. Experimental Brain Research 124, 69-79.

Horslen, B.C., Inglis, J.T., Blouin, J.S., Carpenter, M.G., 2017. Both standing and postural threat decrease Achilles tendon reflex inhibition from tendon electrical stimulation. J Physiol.

Insperger, T., Milton, J., Stepan, G., 2013. Acceleration feedback improves balancing against reflex delay. Journal of the Royal Society, Interface / the Royal Society 10, 20120763.

Kaminski, T.R., Bock, C., Gentile, A.M., 1995. The coordination between trunk and arm motion during pointing movements. Exp Brain Res 106, 457-466.

Kistemaker, D.A., Van Soest, A.J., Wong, J.D., Kurtzer, I., Gribble, P.L., 2013. Control of position and movement is simplified by combined muscle spindle and Golgi tendon organ feedback. J Neurophysiol 109, 1126-1139.

Maaswinkel, E., van Drunen, P., Veeger, H.E., van Dieen, J.H., 2015. Effects of vision and lumbar posture on trunk neuromuscular control. J Biomech 48, 298-303.

Maaswinkel, E., Veeger, H.E., Dieen, J.H., 2014. Interactions of touch feedback with muscle vibration and galvanic vestibular stimulation in the control of trunk posture. Gait Posture 39, 745-749.

Mugge, W., Abbink, D.A., Schouten, A.C., Dewald, J.P., van der Helm, F.C., 2010. A rigorous model of reflex function indicates that position and force feedback are flexibly tuned to position and force tasks. Exp Brain Res 200, 325-340.

Mugge, W., Schuurmans, J., Schouten, A.C., van der Helm, F.C., 2009. Sensory weighting of force and position feedback in human motor control tasks. J Neurosci 29, 5476-5482.

Pigeon, P., Yahia, L.H., Mitnitski, A.B., Feldman, A.G., 2000. Superposition of independent units of coordination during pointing movements involving the trunk with and without visual feedback. Exp Brain Res 131, 336-349.

Pintelon, R., Schoukens, J., 2001. System Identification: A Frequency Domain Approach. John Wiley & Sons, New York, USA.

Sadeghi, S.G., Chacron, M.J., Taylor, M.C., Cullen, K.E., 2007. Neural variability, detection thresholds, and information transmission in the vestibular system. J Neurosci 27, 771-781.

Schafer, S.S., Kijewski, S., 1974. The dependency of the acceleration response of primary muscle spindle endings on the mechanical properties of the muscle. Pflugers Arch 350, 101-122.

Schouten, A.C., De Vlugt, E., Van Hilten, J.J.B., Van der Helm, F.C.T., 2008a. Quantifying proprioceptive reflexes during position control of the human arm. Ieee Transactions on Biomedical Engineering 55, 311-321.

ACCEPTED MANUSCRIPT

Schouten, A.C., Mugge, W., van der Helm, F.C.T., 2008b. NMClab, a model to assess the contributions of muscle visco-elasticity and afferent feedback to joint dynamics. Journal of Biomechanics 41, 1659-1667.

Smith, M., Coppieters, M.W., Hodges, P.W., 2005. Effect of experimentally induced low back pain on postural sway with breathing. Experimental Brain Research 166, 109-117.

Tani, T., Yamamoto, H., Ichimiya, M., Kimura, J., 1997. Reflexes evoked in human erector spinae muscles by tapping during voluntary activity. Electroencephalogr Clin Neurophysiol 105, 194-200.

van der Helm, F.C., Schouten, A.C., de Vlugt, E., Brouwn, G.G., 2002. Identification of intrinsic and reflexive components of human arm dynamics during postural control. J Neurosci Methods 119, 1-14.

van Drunen, P., Koumans, Y., Van der Helm, F.C., van Dieën, J.H., Happee, R., 2015. Modulation of intrinsic and reflexive contributions to low-back stabilization due to vision, task instruction, and perturbation bandwidth. Exp Brain Res 233, 645-749.

van Drunen, P., Maaswinkel, E., van der Helm, F.C., van Dieen, J.H., Happee, R., 2013. Identifying intrinsic and reflexive contributions to low-back stabilization. J Biomech 46, 1440-1446.

van Drunen, P., Maaswinkel, E., van der Helm, F.C.T., van Dieën, J.H., Happee, R., 2014. Corrigendum to “Identifying intrinsic and reflexive contributions to low-back stabilization” [J. Biomech. 46(8) (2013) 1440–1446]. J Biomech 47, 1928-1929.

van Drunen, P., van der Helm, F.C., van Dieën, J.H., Happee, R., 2016. Trunk stabilization during sagittal pelvic tilt: From trunk-on-pelvis to trunk-in-space due to vestibular and visual feedback. J Neurophysiol 115, 1381-1388.

Welch, T.D., Ting, L.H., 2008. A feedback model reproduces muscle activity during human postural responses to support-surface translations. J Neurophysiol 99, 1032-1038.

Welch, T.D., Ting, L.H., 2009. A feedback model explains the differential scaling of human postural responses to perturbation acceleration and velocity. J Neurophysiol 101, 3294-3309.

Willigenburg, N.W., Kingma, I., Hoozemans, M.J., van Dieen, J.H., 2013. Precision control of trunk movement in low back pain patients. Hum Mov Sci 32, 228-239.

Willigenburg, N.W., Kingma, I., van Dieen, J.H., 2010. How is precision regulated in maintaining trunk posture? Experimental Brain Research 203, 39-49.

Willigenburg, N.W., Kingma, I., van Dieen, J.H., 2012. Precision control of an upright trunk posture in low back pain patients. Clinical Biomechanics 27, 866-871.

Yu, X.J., Dickman, J.D., Angelaki, D.E., 2012. Detection thresholds of macaque otolith afferents. J Neurosci 32, 8306-8316.

Zedka, M., Prochazka, A., Knight, B., Gillard, D., Gauthier, M., 1999. Voluntary and reflex control of human back muscles during induced pain. J. Physiol. 520, 591-604.

ACCEPTED MANUSCRIPT

Table 1. Overview of feedback parameters in the models tested. Note that all models contained intrinsic properties as well as MS velocity and position feedback.

	MS				GTO		VES	
model	acceleration gain	velocity gain	position gain	delay	gain	delay	(acceleration) gain	delay
MS		x	x	x				
MS_A	x	x	x	x				
GTO		x	x	x	x	x		
VES		x	x	x			x	x
MS_A+GTO	x	x	x	x	x	x		
MS_A+VES	x	x	x	x			x	x
GTO+VES		x	x	x	x	x	x	x
all	x	x	x	x	x	x	x	x

ACCEPTED MANUSCRIPT

ACCEPTED MANUSCRIPT

Table 2. Parameters that were estimated by model fitting of frequency response functions of admittance and reflexes, with lower and upper bounds used in the estimation procedure.

parameter	lower bound	upper bound
m, effective mass (kg)	10	100
B_C, contact damping (Nsm^{-1})	0	12000
K_C, contact stiffness (Nm^{-1})	5	60000
B_{int}, intrinsic damping (Nsm^{-1}) *	5	2000
K_{eff}, intrinsic stiffness – mg, gravity (Nm^{-1}) *	-2500	12000
K_A, MS acceleration gain (Ns^2m^{-1}) *	-1000	1000
K_V, MS velocity gain (Nsm^{-1}) *	0	6000
K_P, MS position gain (Nm^{-1}) *	0	12000
τ_{MS}, MS delay (ms)	5	70
K_{GTO}, GTO gain (dimensionless) *	-6**	6
τ_{GTO}, GTO delay (ms)	10	100
K_{VES}, VES gain (Ns^2m^{-1}) *	0	5000
τ_{VES}, VES delay (ms)	80	200

MS = muscle spindle; GTO = Golgi tendon organ; VES = vestibular

* indicates that parameters were estimated separately for the relax and resist tasks.

** since negative GTO gains often resulted in model instability, we re-estimated the models containing GTO feedback with a lower boundary on GTO gain of 0.

ACCEPTED MANUSCRIPT

ACCEPTED MANUSCRIPT

Table 3. Overview of significant differences in *VAF* between models. A + symbol marks a significantly higher *VAF* of the model in the left column than the model in the first row; a – symbol marks a significantly lower *VAF* of the model in the left column than the model in the first row and an empty cell indicates no significant difference.

		MS	MS_A	GTO	VES	MS_A+GTO	MS_A+VES	GTO+VES	all
MS_A	adm. relax	+		+	+				–
	adm. resist				–	–			–
	reflex relax	+			+				
	relflex resist	+		+	+		+	+	
GTO	adm. relax		–			–	–	–	–
	adm. resist				+	+	–		–
	reflex relax	+			+				
	relflex resist	+	–		+	–	–		–
VES	adm. relax		–			–	–		–
	adm. resist	+	+	–				+	
	reflex relax		–	–		–	–	–	–
	relflex resist		–	–		–	–	–	–
MS_A+GTO	adm. relax	+		+	+			+	–
	adm. resist		+	–				–	
	reflex relax				+			+	
	relflex resist			+	+		+	+	
MS_A+VES	adm. relax	+		+	+			+	
	adm. resist			+				+	
	reflex relax	+			+				
	relflex resist	+	–	+	+	–			–
GTO+VES	adm. relax			+		–	–		–
	adm. resist				–	+	–		–
	reflex relax	+			+	–			–
	relflex resist	+	–		+	–			–
all	adm. relax	+	+	+	+	+		+	
	adm. resist	+	+	+				+	
	reflex relax	+			+			+	
	relflex resist	+		+	+		+	+	

ACCEPTED MANUSCRIPT

ACCEPTED MANUSCRIPT

Figure 1. a) Experimental set-up, showing the linear actuator applying an anterior directed force to the participant's trunk and the EMG electrodes recording lumbar longissimus muscle EMG. b) Time series of the perturbation force. c) Fourier transform of the perturbation force, showing a single peak for each pair of closely spaced input frequencies.

Figure 2. General structure of the models fitted to the admittance and reflex FRFs. The measured signals, force perturbation ($F_{pert}(t)$), contact force ($F_C(t)$), actuator displacement ($x_A(t)$), and muscle excitation ($E(t)$), are displayed. The dynamics of the actuator H_{env} relates the motor force (F_{pert}) to the actuator displacement (X_A). Trunk stabilisation models (below the dashed line) relate the actuator input to trunk displacement (X_T) based on the dynamics of the trunk mass ($H_m=1/(ms^2)$), intrinsic damping and stiffness ($H_{INT}=bs+k_{eff}$), where k_{eff} represents the lumped effect of trunk stiffness and the negative stiffness due to gravity, contact dynamics ($H_C = b_C s + k_C$), and muscle activation dynamics ($H_{ACT} = (2\pi f_{ACT})^2 / (s^2 + 4\pi f_{ACT} d_{ACT} s + (2\pi f_{ACT})^2)$). Muscle spindle feedback was described by acceleration, velocity and position feedback ($H_{MS} = (k_A s^2 + k_V s + k_P) e^{-\tau_{MS} s}$) of which the acceleration feedback component k_A was used in specific models only. Some models included force feedback by Golgi tendon organs ($H_{GTO} = k_F e^{-\tau_{GTO} s}$) and/or vestibular feedback ($H_{VEST} = k_{VES} s^2 e^{-\tau_{ves} s}$).

Figure 3. Boxplots of Variance Accounted For (VAF) in the time series of trunk displacement (admittance, left) and EMG amplitude modulation (reflex, right) for the relax (top)and resist (bottom) tasks for all models. Symbols indicate median (red line), interquartile range (blue box), extremes (black whiskers) and outliers (red +). Outliers are defined as larger than $q_3 + 1.5(q_3 - q_1)$ or smaller than $q_1 - 1.5(q_3 - q_1)$, where q_1 and q_3 are the 25th and 75th percentiles (marked by the blue boxes), respectively. See Table 2 for model properties and Table 3 for significant differences between models.

Figure 4. Boxplots of estimates of reflex delays for all models. Symbols indicate median (red line), interquartile range (blue box), extremes (black whiskers) and outliers (red +). Outliers are defined as larger than $q_3 + 1.5(q_3 - q_1)$ or smaller than $q_1 - 1.5(q_3 - q_1)$, where q_1 and q_3 are the 25th and 75th percentiles (marked by the blue boxes), respectively. The shaded areas indicate the boundraies used in the optimization. See Table 2 for model properties.

Figure 5. Typical example of the empirical and modeled FRFs (a) and reconstructed time series (b) of trunk displacement and muscle excitation for the relax task for a single subject. Empirical data (black line), optimized MS model (blue line) and optimized MS_A model (red line). For comparability to model data empirical time series were Fourier transformed and inverse transformed.

Figure 6. a) Frequency response functions of the admittance and reflexes derived from MS_A models for the resist task. b) Time domain representations of the model predicted trunk displacement and modulation of muscle excitation for the resist task. In all graphs, thick red lines represent predictions based on median estimates of all model parameters, thin orange and green lines represent model predictions based on the 25^{th} and 75^{th} percentile estimates of acceleration feedback gains, respectively with all other estimates at median values, and black dashed lines represent predictions of an MS model (zero acceleration feedback gain) with the median delay (37.3 ms) of the MS_A model.

ACCEPTED MANUSCRIPT

supplementary material

Figure S.1. Boxplots of estimates of reflex gains for all models. Symbols indicate median (red line), interquartile range (blue box), extremes (black whiskers) and outliers (red +). Outliers are defined as larger than $q_3 + 1.5(q_3 - q_1)$ or smaller than $q_1 - 1.5(q_3 - q_1)$, where q_1 and q_3 are the 25th and 75th percentiles (marked by the blue boxes), respectively. See Table 2 for model properties.

Figure S.2. Boxplots of estimates of intrinsic model parameters (intrinsic damping, intrinsic stiffness) and contact dynamics (damping and stiffness) for all models. Symbols indicate median (red line), interquartile range (blue box), extremes (black whiskers) and outliers (red +). Outliers are defined as larger than $q_3 + 1.5(q_3 - q_1)$ or smaller than $q_1 - 1.5(q_3 - q_1)$, where q_1 and q_3 are the 25th and 75th percentiles (marked by the blue boxes), respectively. See Table 2 for model properties.

Figure S.3. Boxplots of estimates of upper body mass (anthropometric estimate (0.58 body mass) and effective mass for all models. For each model, Pearson's correlation of effective mass with the anthropometrical estimate of body mass is given. Symbols indicate median (red line), interquartile range (blue box), extremes (black whiskers) and outliers (red +). Outliers are defined as larger than $q_3 + 1.5(q_3 - q_1)$ or smaller than $q_1 - 1.5(q_3 - q_1)$, where q_1 and q_3 are the 25th and 75th percentiles (marked by the blue boxes), respectively. See Table 2 for model properties.

ACCEPTED MANUSCRIPT

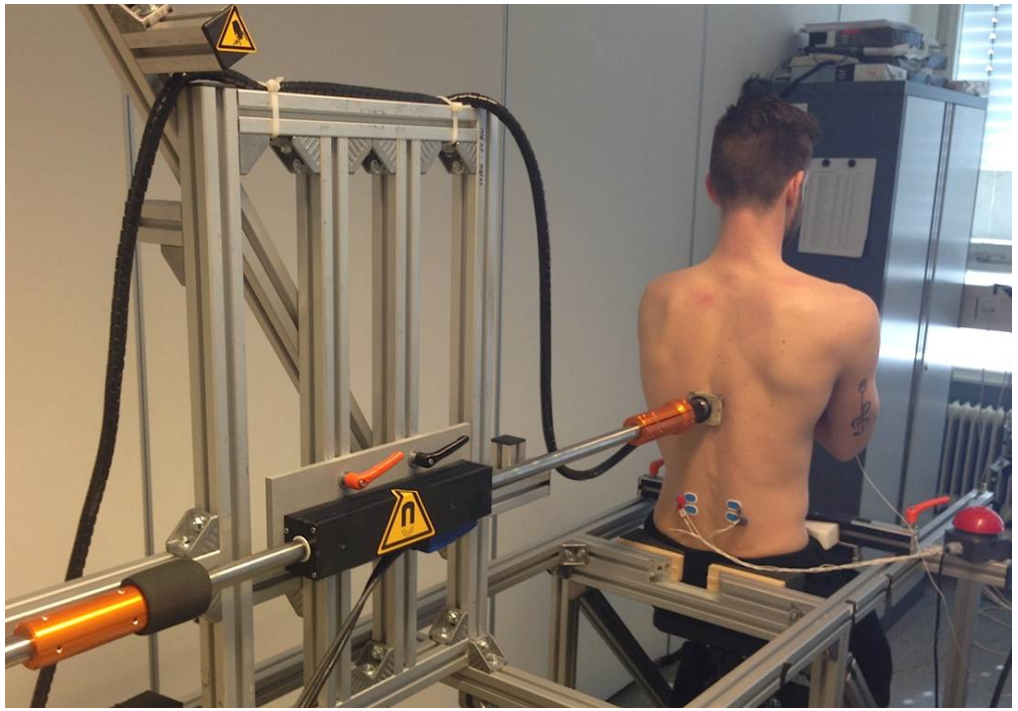

a

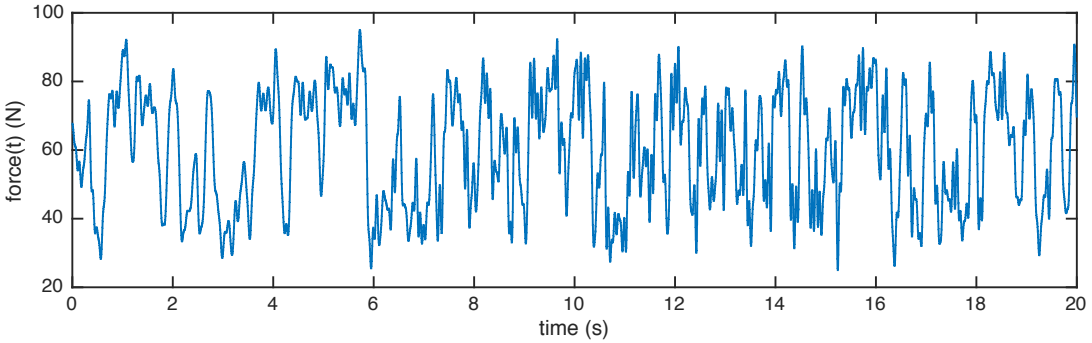

b

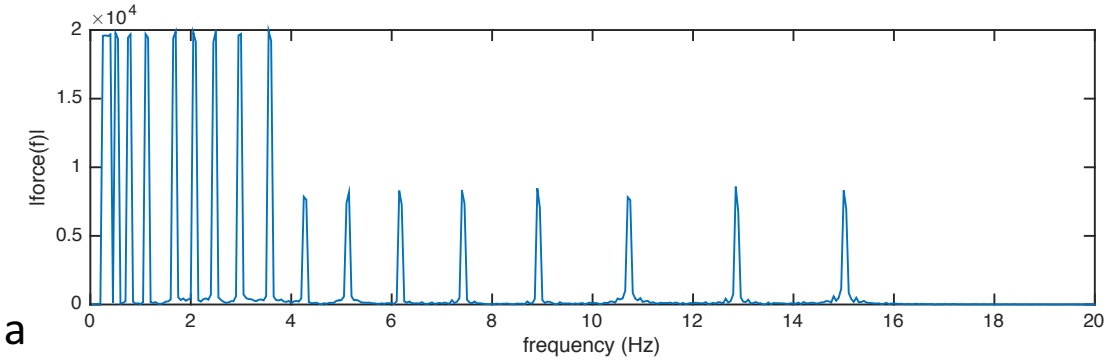

c

Fig. 1

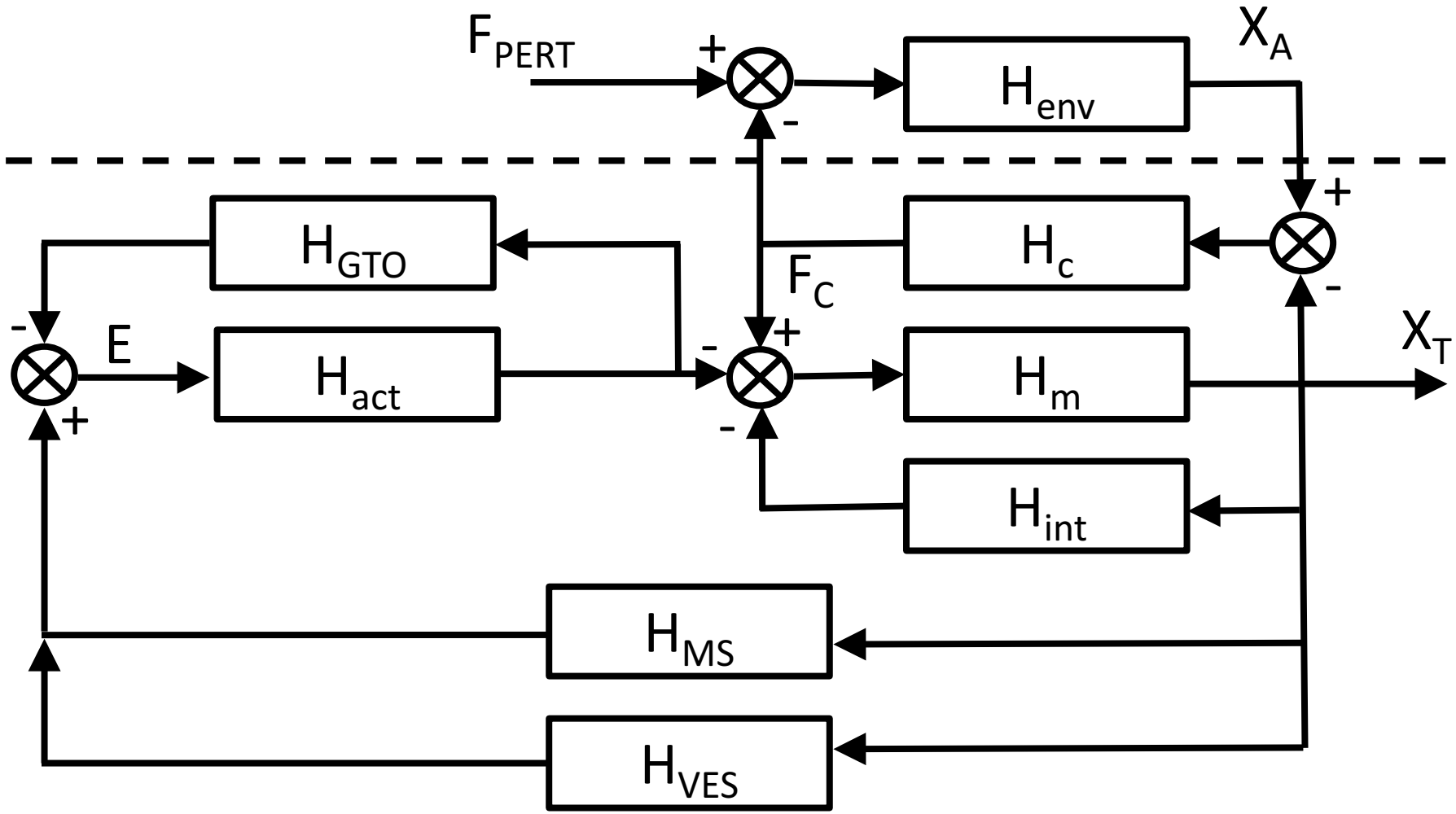

Fig. 2

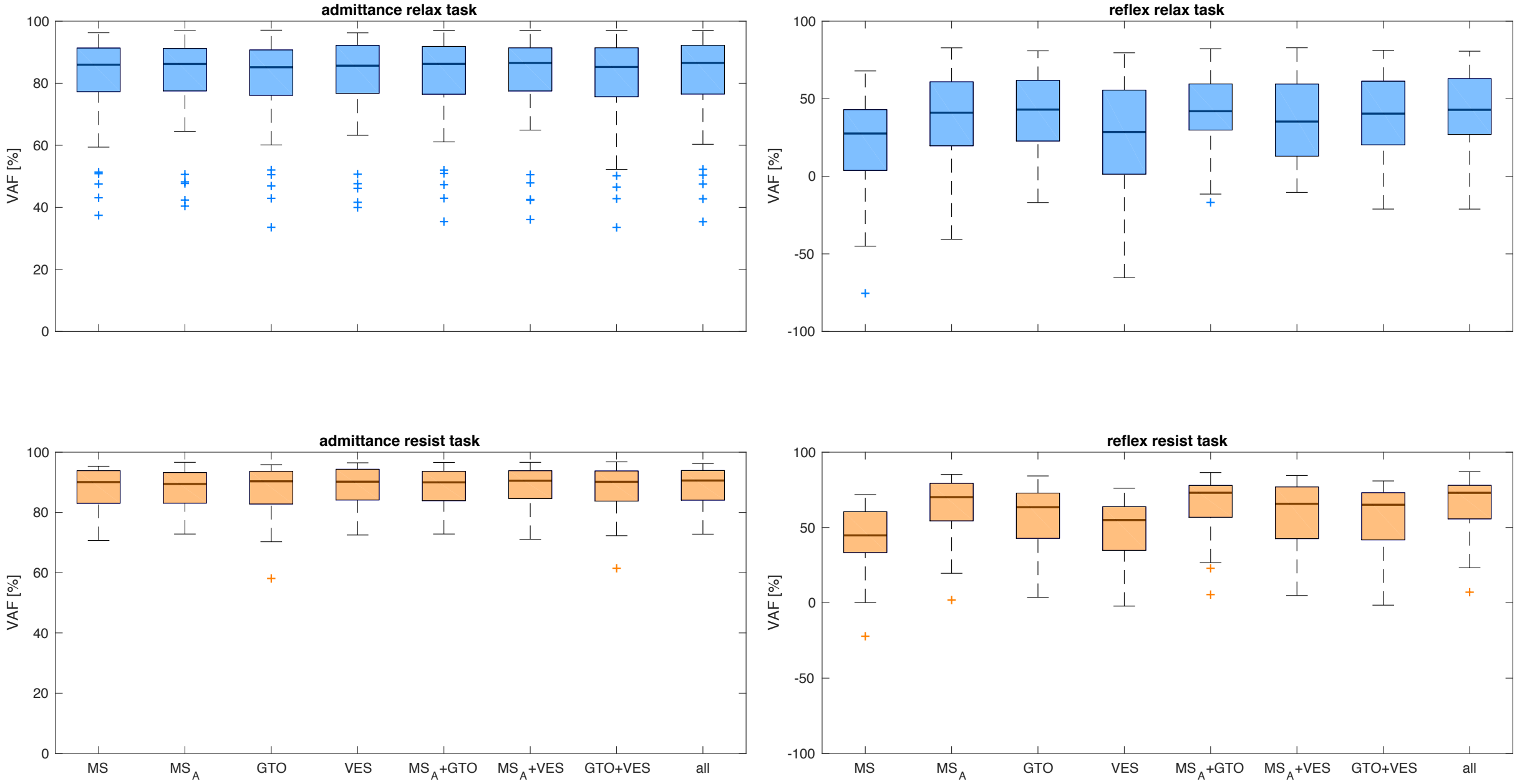
admittance relax task
reflex relax task
admittance resist task
reflex resist task
VAF [%]
100
80
60
40
20
0
50
-50
-100
MS
MS A
GTO
VES
MS A +GTO
MS A +VES
GTO+VES
all

Fig. 3

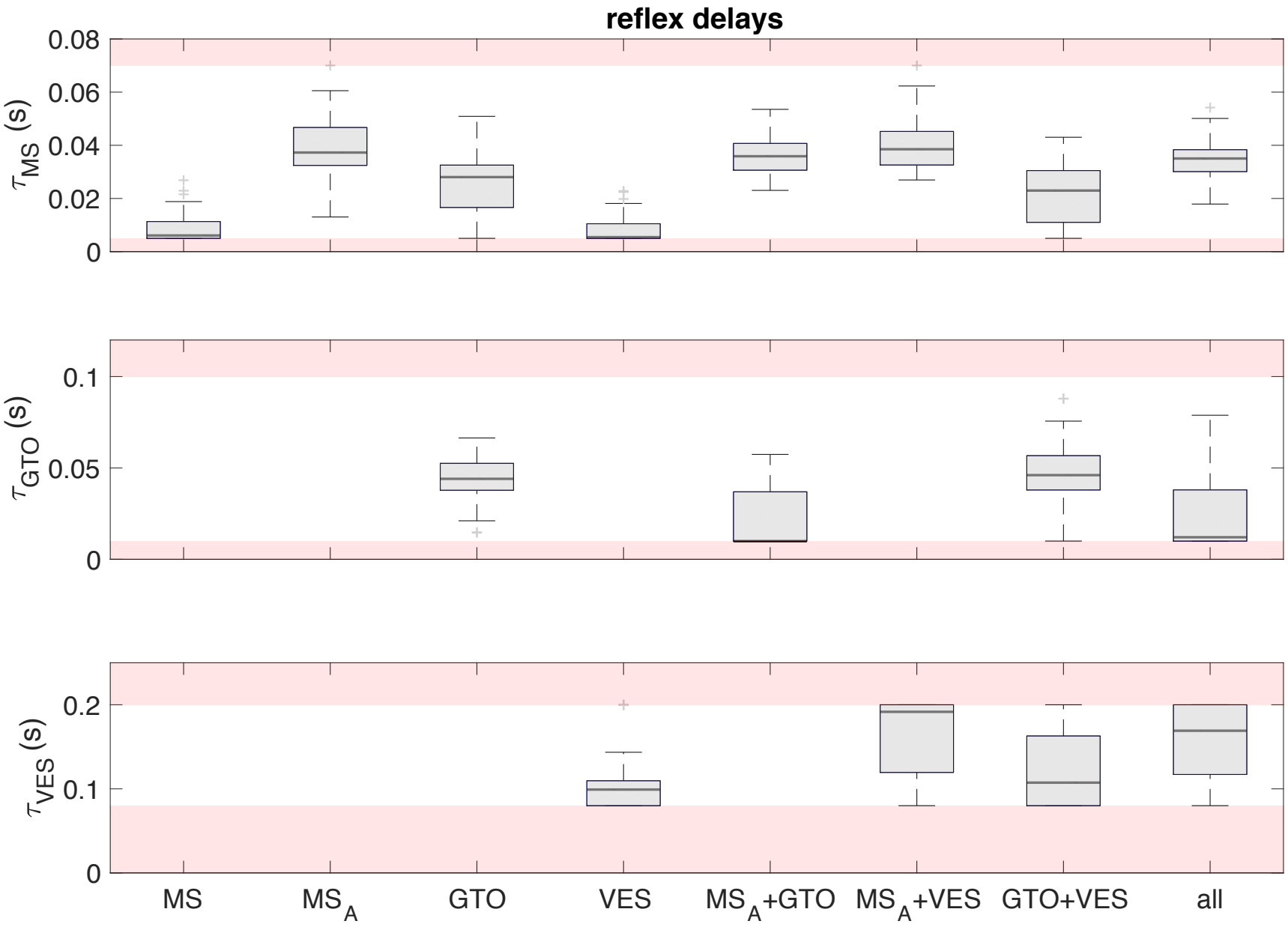
reflex delays
0.08
0.06
0.04
0.02
0
τ_{MS} (s)
0.1
0.05
0
τ_{GTO} (s)
0.2
0.1
0
τ_{VES} (s)
MS
MS_A
GTO
VES
MS_A+GTO
MS_A+VES
GTO+VES
all

Fig. 4

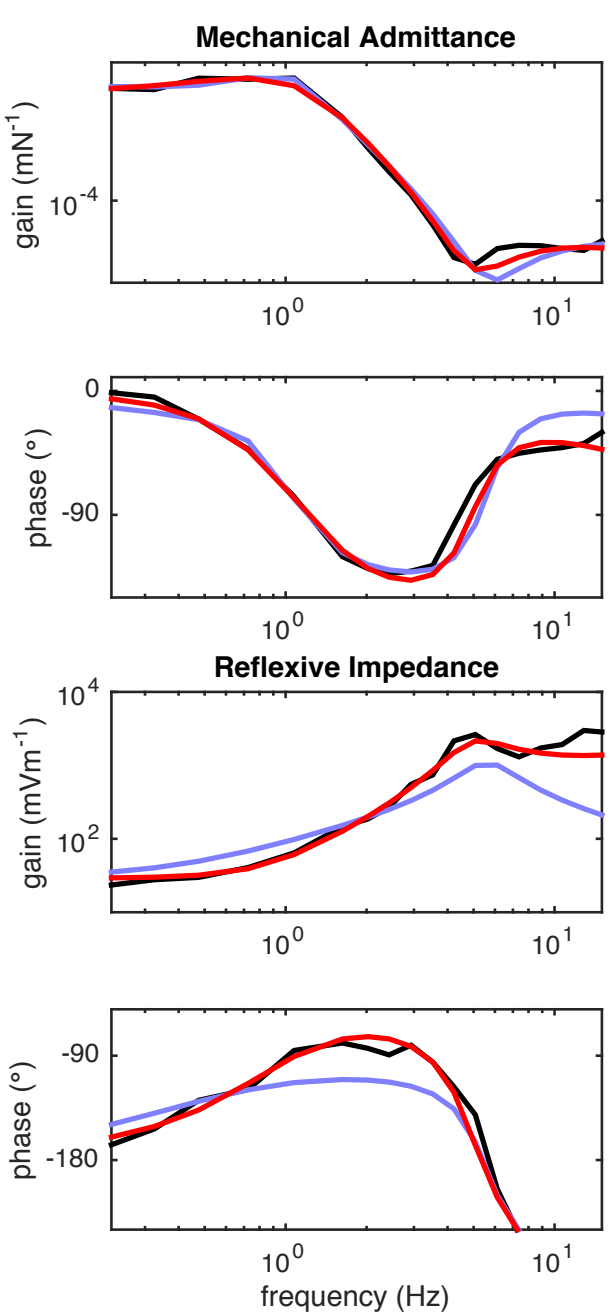
Mechanical Admittance
gain (mN-1)
10-4
100
101
phase (°)
0
-90
100
101
Reflexive Impedance
gain (mVm-1)
104
102
100
101
phase (°)
-90
-180
100
101
frequency (Hz)

a

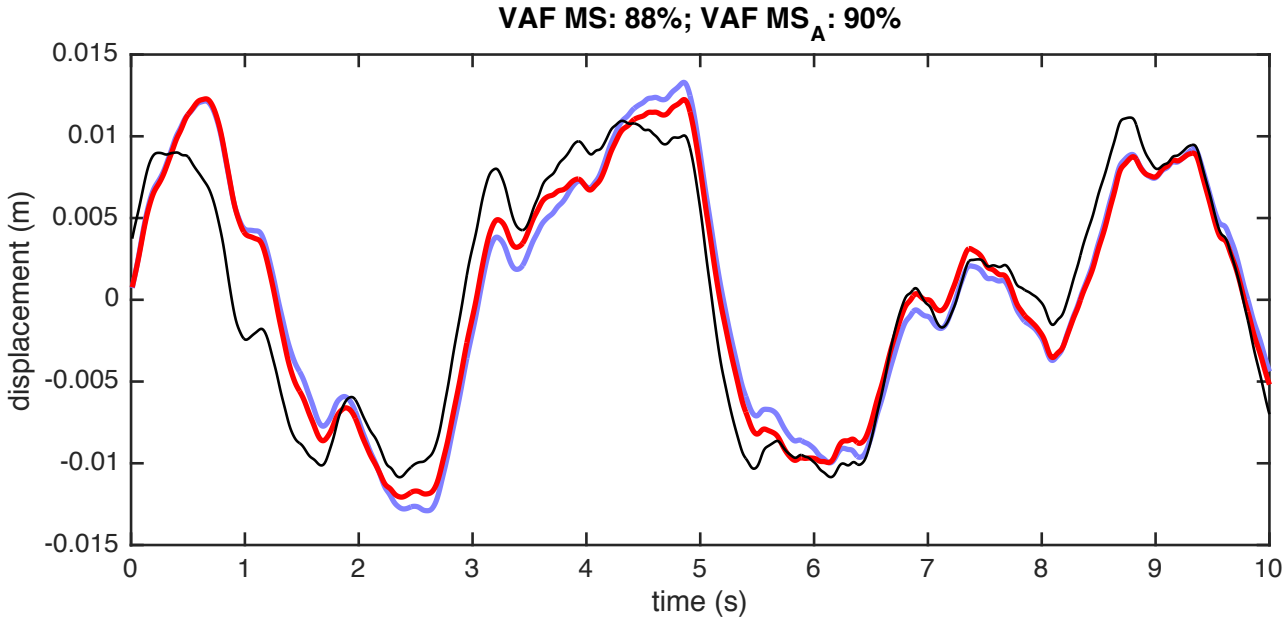
VAF MS: 88%; VAF MSA: 90%
displacement (m)
0.015
0.01
0.005
0
-0.005
-0.01
-0.015
0
1
2
3
4
5
6
7
8
9
10
time (s)

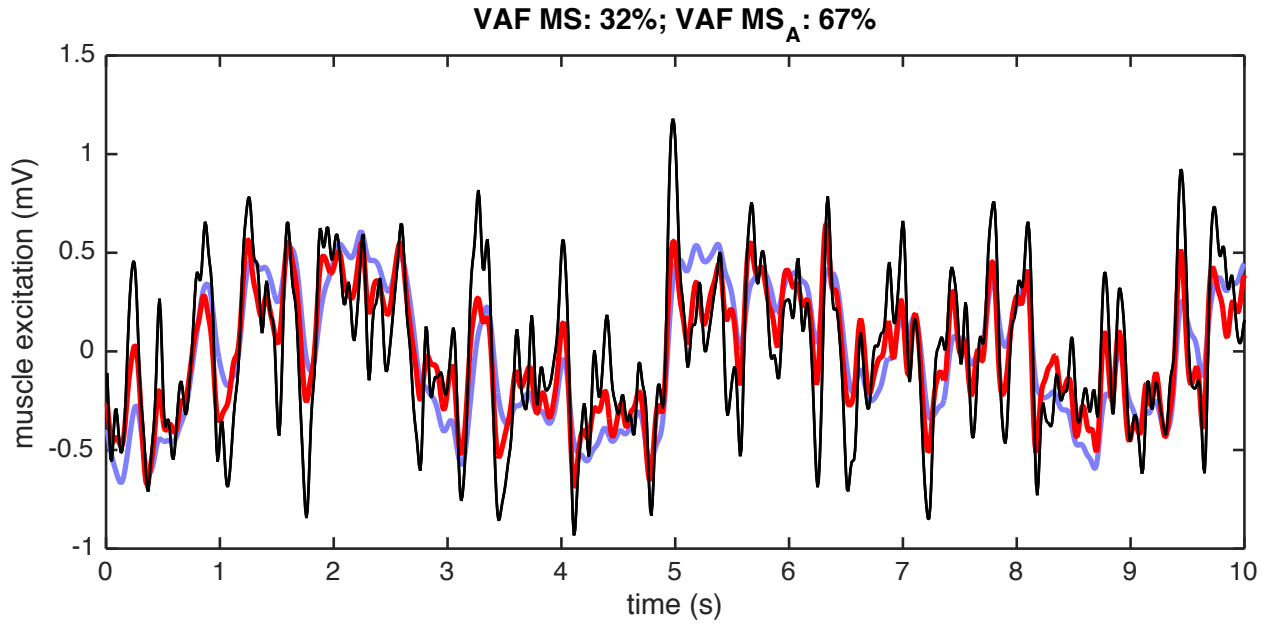
VAF MS: 32%; VAF MSA: 67%
muscle excitation (mV)
1.5
1
0.5
0
-0.5
-1
0
1
2
3
4
5
6
7
8
9
10
time (s)

b

Fig. 5

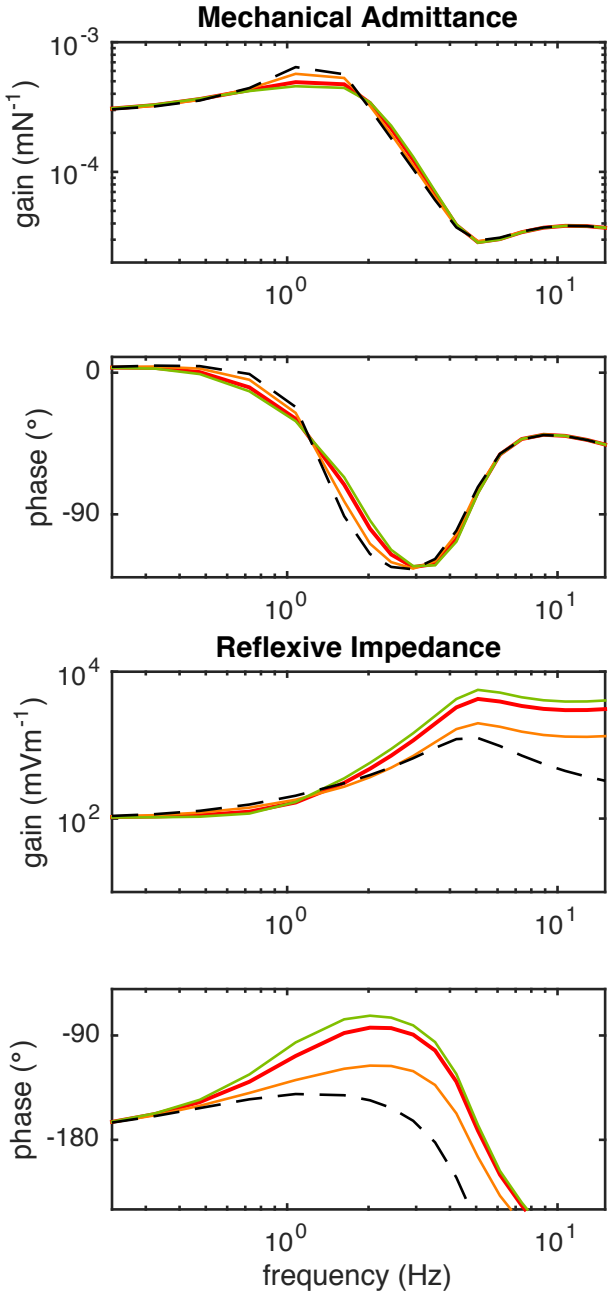
Mechanical Admittance
gain (mN-1)
phase (°)
Reflexive Impedance
gain (mVm-1)
phase (°)
frequency (Hz)

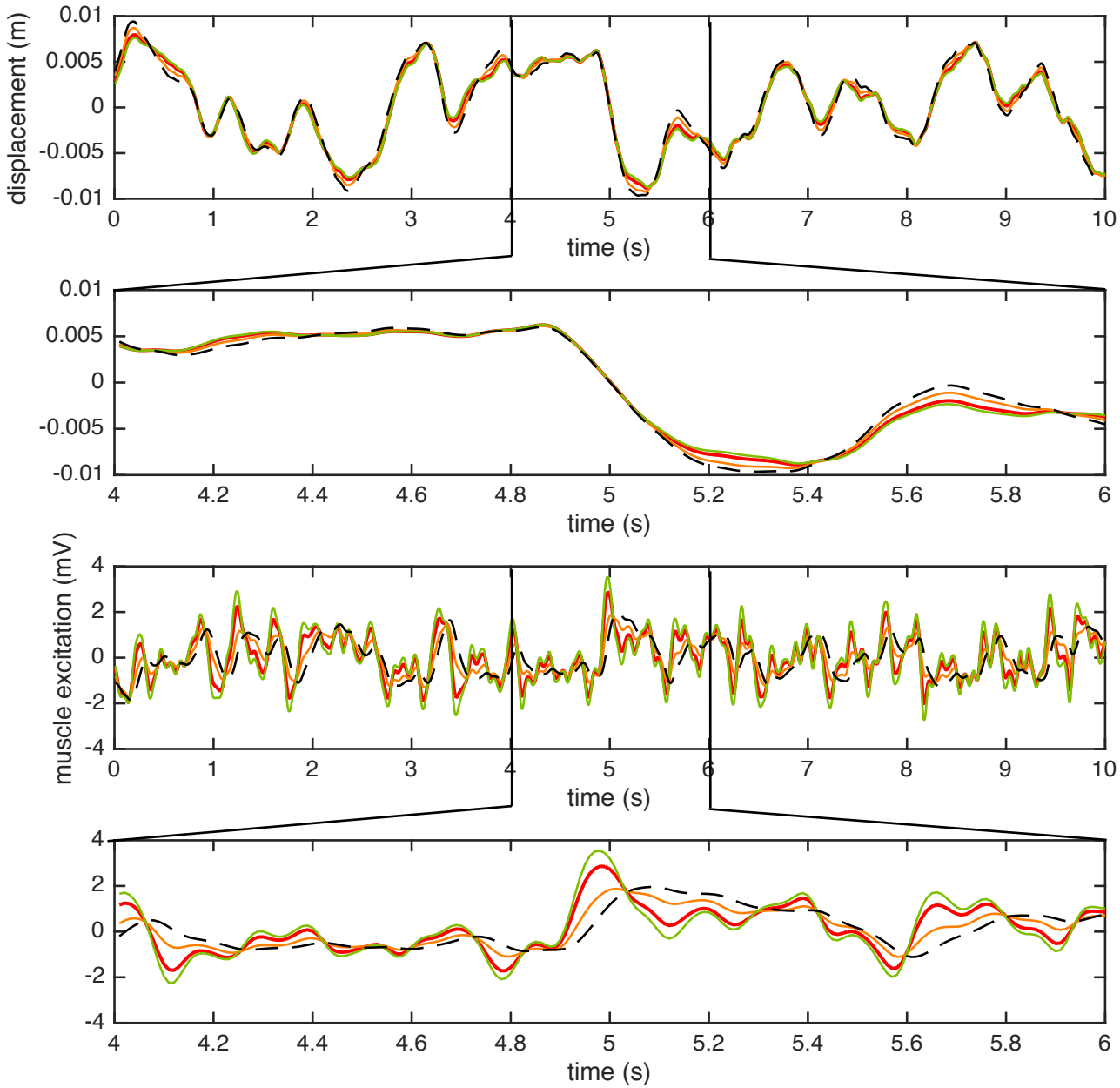
displacement (m)
time (s)
muscle excitation (mV)
time (s)

Fig. 6

a

b

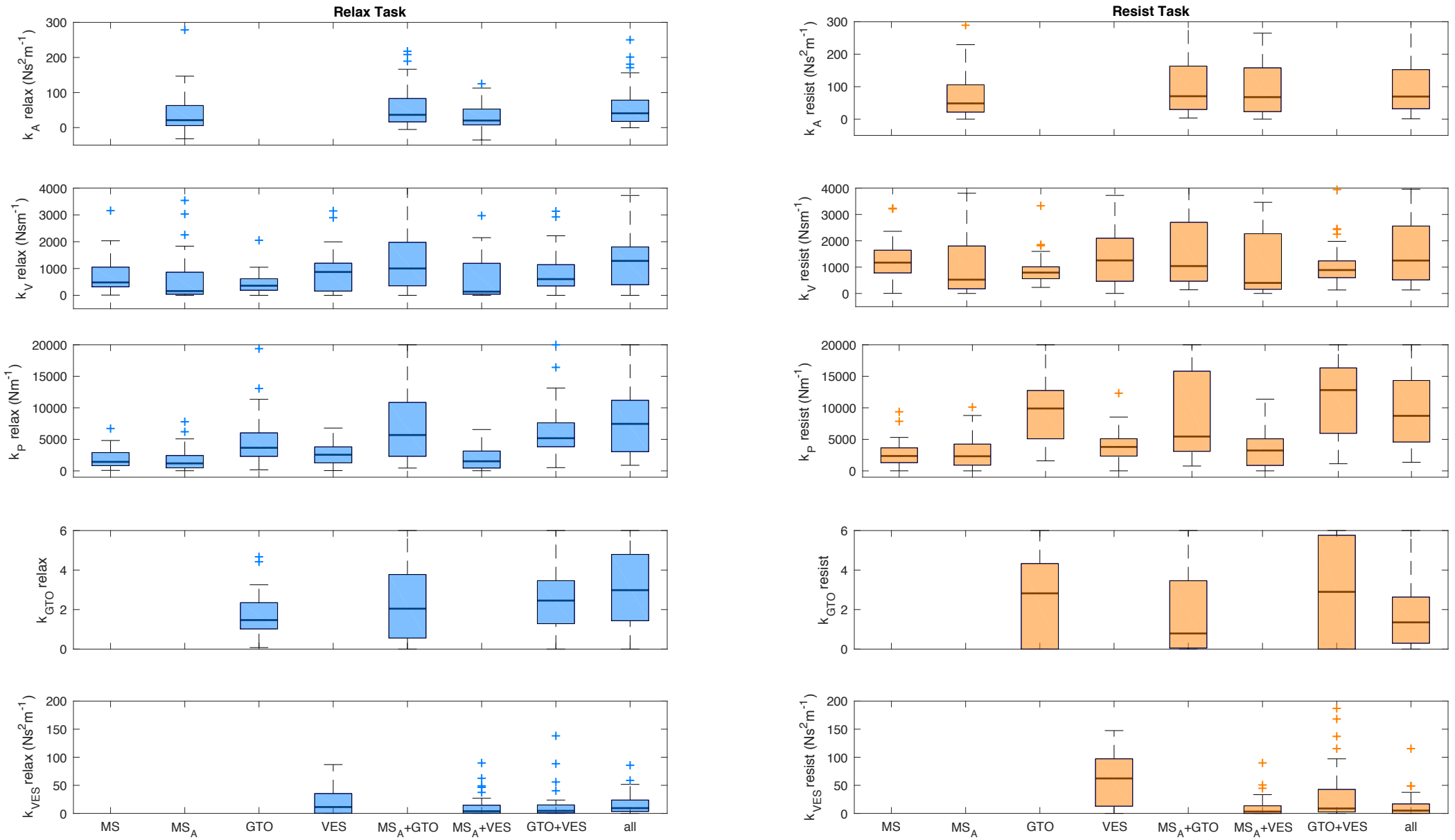
Relax Task
Resist Task
k_A relax (Ns^2m^{-1})
k_A resist (Ns^2m^{-1})
k_V relax (Nsm^{-1})
k_V resist (Nsm^{-1})
k_P relax (Nm^{-1})
k_P resist (Nm^{-1})
k_{GTO} relax
k_{GTO} resist
k_{VES} relax (Ns^2m^{-1})
k_{VES} resist (Ns^2m^{-1})
MS
MS_A
GTO
VES
MS_A+GTO
MS_A+VES
GTO+VES
all

Fig. S.1

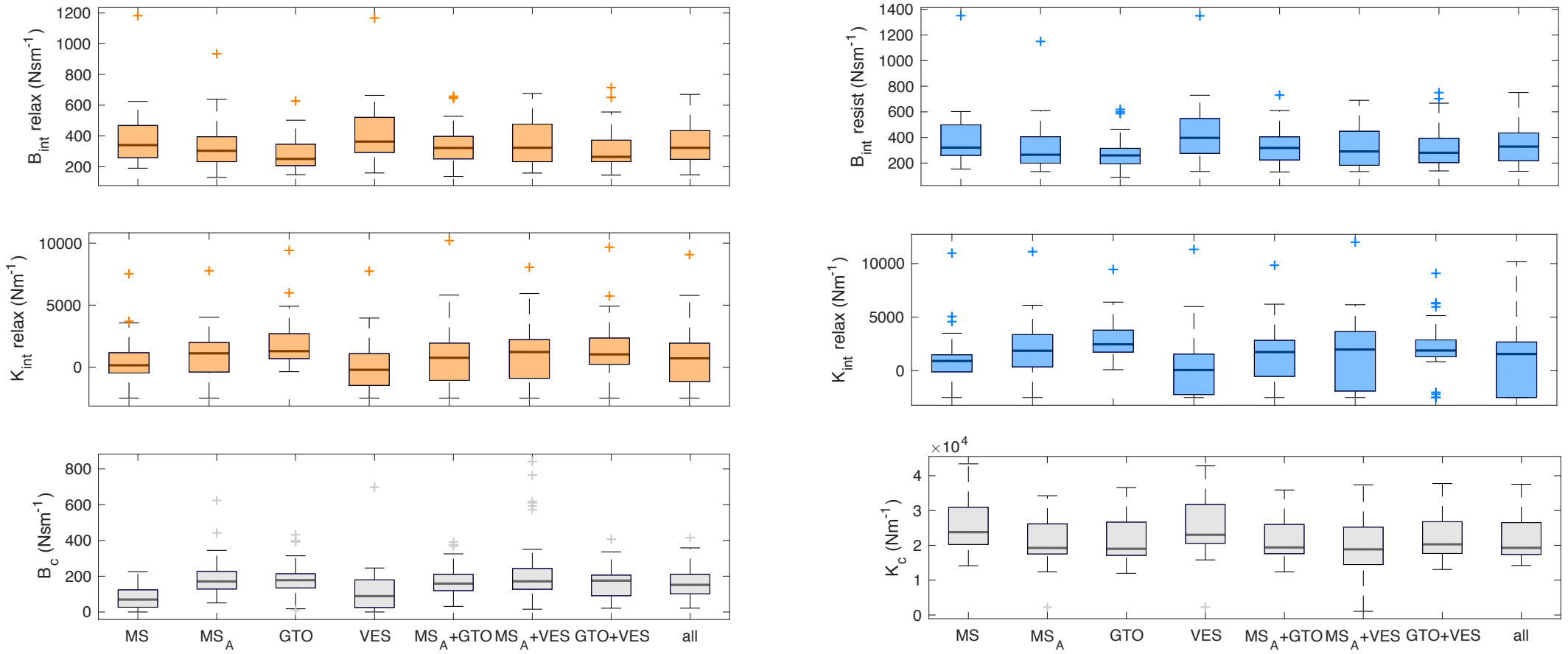
B_int relax (Nsm^-1)
1200
1000
800
600
400
200
K_int relax (Nm^-1)
10000
5000
0
B_c (Nsm^-1)
800
600
400
200
0
MS
MS_A
GTO
VES
MS_A+GTO
MS_A+VES
GTO+VES
all
B_int resist (Nsm^-1)
1400
1200
1000
800
600
400
200
K_int relax (Nm^-1)
10000
5000
0
×10^4
K_c (Nm^-1)
4
3
2
1
0
MS
MS_A
GTO
VES
MS_A+GTO
MS_A+VES
GTO+VES
all

Fig. S.2

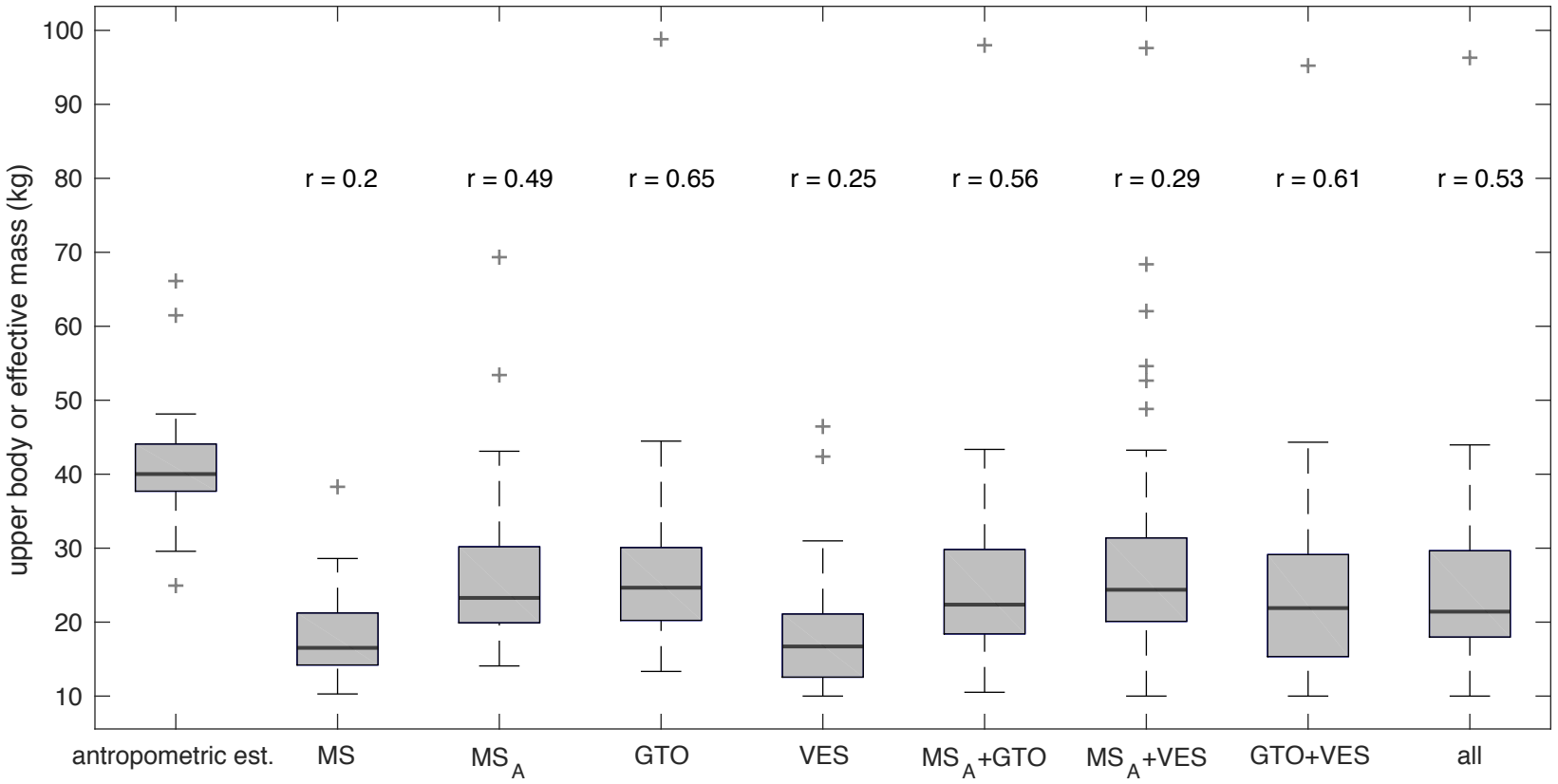
upper body or effective mass (kg)
100
90
80
70
60
50
40
30
20
10
r = 0.2
r = 0.49
r = 0.65
r = 0.25
r = 0.56
r = 0.29
r = 0.61
r = 0.53
antropometric est.
MS
MS A
GTO
VES
MS A +GTO
MS A +VES
GTO+VES
all

Fig. S.3